*Animal* (2010), **4:9**, pp 1613–1617 © The Animal Consortium 2010
doi:10.1017/S1751731110000698

animal

# Effects of frozen storage temperature on the elasticity of tendons from a small murine model

K. L. Goh[1†], Y. Chen[2], S. M. Chou[3], A. Listrat[4], D. Bechet[5] and T. J. Wess[6]

[1]*School of Engineering, Monash University, 46150, Selangor Darul Ehsan, Malaysia;* [2]*School of Chemical & Biomedical Engineering, Nanyang Technological University, 637459, Singapore;* [3]*School of Mechanical & Aerospace Engineering, Nanyang Technological University, 639798, Singapore;* [4]*Growth and Muscle Metabolism Laboratory, Institut National de la Recherche Agronomique, 63122 St Genes-Champanelle, France;* [5]*Human Nutrition Research Center, Institut National de la Recherche Agronomique, 63122 St Genes-Champanelle, France;* [6]*School of Optometry & Vision Sciences, Cardiff University, Cardiff, CF24 4LU, UK*

(Received 7 September 2009; Accepted 25 February 2010; First published online 26 April 2010)

*The basic mechanism of reinforcement in tendons addresses the transfer of stress, generated by the deforming proteoglycan (PG)-rich matrix, to the collagen fibrils. Regulating this mechanism involves the interactions of PGs on the fibril with those in the surrounding matrix and between PGs on adjacent fibrils. This understanding is key to establishing new insights on the biomechanics of tendon in various research domains. However, the experimental designs in many studies often involved long sample preparation time. To minimise biological degradation the tendons are usually stored by freezing. Here, we have investigated the effects of commonly used frozen storage temperatures on the mechanical properties of tendons from the tail of a murine model (C57BL6 mouse). Fresh (unfrozen) and thawed samples, frozen at temperatures of −20°C and −80°C, respectively, were stretched to rupture. Freezing at −20°C revealed no effect on the maximum stress ($\sigma$), stiffness (E), the corresponding strain ($\varepsilon$) at $\sigma$ and strain energy densities up to $\varepsilon$ (u) and from $\varepsilon$ until complete rupture ($u_p$). On the other hand, freezing at −80°C led to higher $\sigma$, E and u; $\varepsilon$ and $u_p$ were unaffected. The results implicate changes in the long-range order of radially packed collagen molecules in fibrils, resulting in fibril rupture at higher stresses, and changes to the composition of extrafibrillar matrix, resulting in an increase in the interaction energy between fibrils via collagen-bound PGs.*

**Keywords:** frozen storage temperature, strength, stiffness, strain energy, collagen

## Implications

Ultra-low storage temperature alters (i) the long-range order of collagen packing in fibrils, resulting in fibril rupture at higher stresses, and (ii) the composition of extra-fibrillar matrix, resulting in an increase in the interaction energy between fibrils via collagen-bound proteoglycans. Consequently, the tissue strength, stiffness and fracture toughness increase.

## Introduction

This study is concerned with the effects of frozen storage temperature on the elasticity of tendons, which are biological examples of fibre-reinforced composites comprising highly paralleled collagen fibrils embedded in the hydrated proteoglycan (PG)-rich extracellular matrix (ECM; Hukins and Aspden, 1985; Figure 1a). The basic mechanism of reinforcement in tendons addresses the transfer of stress generated in the deforming PG-rich matrix, in response to an external load, to the collagen fibrils (Goh *et al.*, 2005). Regulating this mechanism involves the interactions of PGs on the fibrils with those in the surrounding matrix and between adjacent fibrils (Goh *et al.*, 2007). The stress transfer mechanism is fundamental to understanding the biomechanics of load transmission, from muscle to bone by tendons, in many studies. These studies may be found in biomedical science, for example, addressing the biomarkers of ageing (Derwin and Soslowsky, 1999), injury and repair (Lin *et al.*, 2004), and meat science, for example, investigating the mechanical response in relation to the quality of the attachment of muscle to bone from livestock (Moussa *et al.*, 2007; Gondret *et al.*, 2009). Unfortunately, experimental designs in these studies often involve long sample preparation time. To minimise biological degradation, tendons are stored by freezing, usually at around −20°C (Moussa *et al.*, 2007; Goh *et al.*, 2008; Gondret *et al.*, 2009) or at ultra-low temperatures, for example, −80°C (Giannini *et al.*, 2008), until the day of testing. Although the processes that regulate the formation of ice crystallites and the disruption of cells and ECM

† E-mail: goh.kheng.lim@eng.monash.edu.my

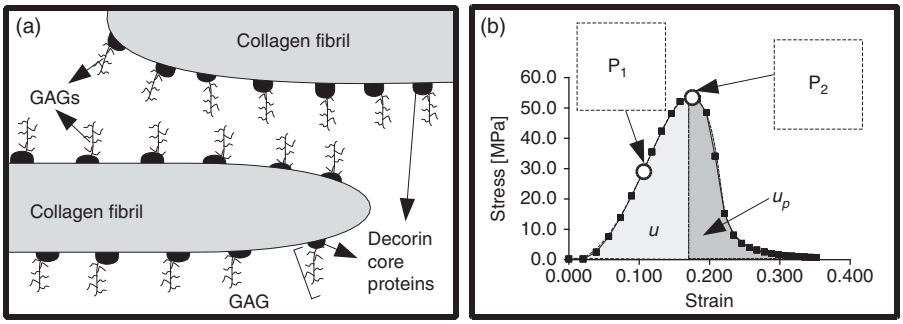


**Figure 1** (a) Extracellular matrix of tendons comprising of collagen fibrils embedded in a hydrated PG-rich matrix. Decorin core proteins, with glycosaminoglycans (GAGs) attached, are depicted on the surface of collagen fibrils. (b) A stress-strain curve (M20) illustrating the areas under the curve corresponding to the strain energy density to maximum stress ($u$) and to fracture ($u_p$); arrows P1 and P2 indicate the point of inflexion and the maximum stress ($\sigma$) point, respectively.

organisation are well-known (Muldrew and McGann, 1990), how frozen storage temperature affects the basic mechanisms that regulate the ECM elasticity, leading to changes in the mechanical properties, is not clear.

We have investigated the influence of frozen storage temperatures on the mechanical properties of tendons from the tail of a small murine model (C57BL6 mouse). Here, we are concerned with the maximum stress, $\sigma$, on the stress-strain curve, stiffness ($E$), strain ($\varepsilon$) at $\sigma$, strain energy densities up to $\varepsilon$ ($u$) and from $\varepsilon$ until complete rupture ($u_p$) (Goh *et al.*, 2005). Since the genome of the C57BL6 mouse has been sequenced, it has been regarded as an ideal murine model in the context of integrative biology study; it is widely used for laboratory experiments to illuminate basic mechanisms that could address similar outcomes in other mammals (Laissue *et al.*, 2009). In particular, tissues from the murine model have been used extensively to evaluate biomechanical properties to study systemic changes caused by injury and during healing (Lin *et al.*, 2004), ageing of ECM (Goh *et al.*, 2008) and disruption of the signal pathway for regulating ECM in genetically engineered mice that produced alterations in collagen (Derwin and Soslowsky, 1999) and PGs (Derwin and Soslowsky, 1999). Application of the principles of fibre-reinforced composites to connective tissues such as tendons has yielded insights on the mechanisms of elastic and plastic stress transfers in collagen fibrils and on fibril–fibril interactions across the hydrated PG-rich matrix within ECM for regulating tissue elasticity (Goh *et al.*, 2005). Here, these insights will be used to speculate on the sensitivity of these mechanisms to low storage temperatures.

## Material and methods

*Sample preparation*

Tendons, of about 200 μm thick, were dissected from the tail of a 16-month-old mouse (C57BL6) which was killed in accordance with the procedure laid down by the National Research Council for the care and use of laboratory animals. The tendons were transected and divided equally into three groups consisting of ten samples per group. One group was designated as control and was tested immediately. Samples from the second (M20) and third (M80) groups were immediately placed in freezers operating at −20°C (MDF-U5411, Sanyo, Osaka, Japan) and −80°C (MDF-U73V, Sanyo), respectively. After 24 h, the frozen samples were thawed at room temperature for analysis.

*Mechanical tests*

A small-scale horizontal tensile rig, designed and built in-house, was used for mechanical tests (Goh *et al.*, 2008). Each sample was mounted onto the rig, secured by the grips at its ends and hydrated by submerging in phosphate buffered saline, pH 7.2, at room temperature. The rig was mounted onto an inverted microscope (DM-IL, Leica Microsystems GmbH, Wetzlar, Germany) for sample observation during the test. A displacement rate of 0.067 mm/s was applied to stretch the sample until the tissue ruptured (Goh *et al.*, 2008). The force generated in the sample was recorded by a load cell (UF-1, Pioden Controls Ltd) coupled to one grip; the sample extension corresponded to the relative displacement of the grips, which was recorded by a linear variable displacement transducer (CDP-M, Tokyo Sokki Kenkyujo, Tokyo, Japan).

*Determination of mechanical properties*

Stress-strain plots were obtained from the load-extension data. Here, stress is defined as the ratio of the load to the nominal cross-sectional area of the sample; strain is the ratio of the change in the sample length to the length described by the grip-to-grip distance. By fitting an appropriate polynomial equation to the data points on the plot, from stress = 0 to $\sigma$, the point of inflexion was identified (Figure 1b). The gradient at this point parameterised $E$ (Goh *et al.*, 2008).

From the area under the stress-strain curve (Figure 1b), the strain energy density ($u$) up to $\sigma$ was evaluated to determine the energy needed to cause tissue failure; in this region the energy absorbed is dominated by fibril recruitment and fibril yielding (Goh *et al.*, 2008). We have also determined the strain energy density $u_p$, from $\varepsilon$ until when the tissue ruptured completely, to account for the energy absorbed by the dominant failure modes, namely fibril pull-out by frictional sliding at the fibril–PG matrix interface, as well as PG matrix rupture (Sikoryn and Hukins, 1988).

*Statistical analyses*

Representative (mean ± s.e.) values of the mechanical parameters, that is, $\sigma$, $E$, $\varepsilon$, $\varepsilon_y$ and $u$, for each treatment were determined. Paired sample $t$-test was used to analyse for differences between the control *v.* each treatment group at $\alpha = 0.05$. Differences due to the treatment were considered significant if the $P$-value was $< 0.05$.

## Results

Figure 2 shows stress-strain plots derived from the control, M20 and M80 groups. In general, during the loading stage, all samples featured a toe region followed by a rapid increase in the rate of change of stress with respect to strain; during tissue failure, that is beyond the strain at maximum stress, the gradients decreased rapidly until rupture. Of the three groups, the M80 group yielded the largest gradient during the loading stage and during tissue failure.

Examination of the microstructure of tendons from the control, M20 and M80 groups revealed wavy collagen fibres (which are one hierarchy above collagen fibrils) that exhibited the usual structural changes, that is de-crimping and straightening (Figure 3a), during loading. All the three groups responded with similar structural changes during mechanical loading. Immediately after $\sigma$, the tendon began to fail (Figure 3b). Here, a thin section bridging the bulk of tissue was observed (arrow A). Rupture and pull-out of collagen fibres were also observed; the ends of these structures are indicated by arrow B. At the lower hierarchical level, this could implicate collagen fibril rupture and pull-out. Longitudinal splits in the tendon were also observed, implicating the rupture of the PG matrix (arrow C).

The results of $\sigma$, $E$, $\varepsilon$, $u_p$ and $u$ for the control, M20 and M80 groups are listed in Table 1. In all the cases considered here, no significant difference was observed between the control and M20 groups. No significant difference was observed between the control and M80 groups for $\varepsilon$ and $u_p$. However, the M80 group yielded magnitudes of $\sigma$, $E$ and $u$, which were 1.4, 1.5 and 1.6 times significantly higher, respectively, than the control group.

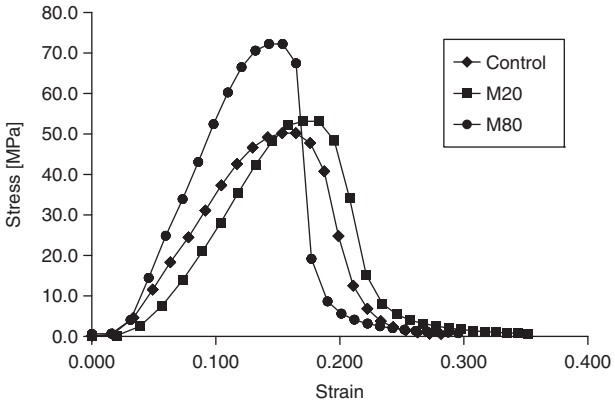


**Figure 2** Plot of stress *v.* strain from control and treated samples. Data points represent a typical experiment from one sample each.

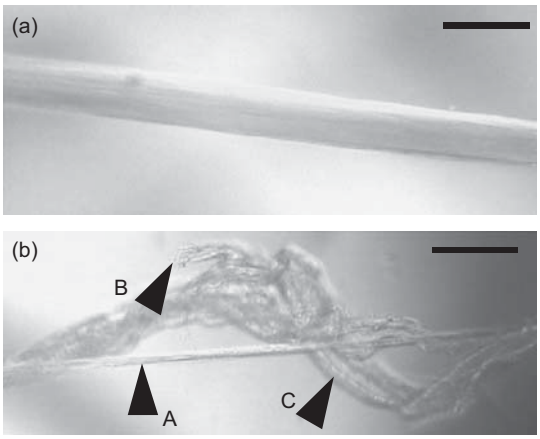


**Figure 3** Microscopic examination of tendon samples (a) during initial loading, (b) post-peak stress, $\sigma$. The images in part (a) and (b) were taken from a sample belonging to the M20 (samples treated at −20°C) group. Horizontal (scale) bar has a length of 100 μm. Arrow A indicates a thin section bridging the bulk of tissue. Arrow B indicates the ends of the fibres. Arrow C indicates longitudinal splits in the tendon.

## Discussion

Collagen fibrils feature a crystalline arrangement of collagen molecules. This crystalline arrangement is characterised by a long-range order of radially packed (side-to-side) collagen molecules and an ordered array of axially staggered collagen molecules along the fibril axis (Laing *et al.*, 2003). The long-range order characterises the crystalline system in which portions deep within the fibril, that is, far from the fibril–PG matrix interface, exhibit similar strain response; strain energy will not concentrate at the interface but will eventually be absorbed by molecules at greater depths from the interface. Decorin PGs associated with the collagen fibrils consist of a core protein, bound to collagen, with a side chain known as glycosaminoglycans (GAGs; Figure 1; Screen *et al.*, 2006). The non-steric interactions between GAGs, from the respective decorin PGs on adjacent fibrils, is implicated for regulating the stress transfer to collagen fibrils as the fibrils slide relative to one another when the tissue is loaded (Screen *et al.*, 2006; Goh *et al.*, 2007). According to the elasticity of materials (Sun, 2009), it follows that $E$ and $\sigma$ may be determined by equilibrating the external mechanical load to the responses of the intermolecular forces of the tendons. Thus,

$$E \propto U_1/V \quad (1)$$

$$\sigma \propto U_2/V \quad (2)$$

where $U_1$ and $U_2$ are the sum of cohesive energy per bond, at equilibrium between the biomacromolecules, within a volume, $V$ (Sun, 2009). Although $E$ and $\sigma$ have similar dimensions, the molecular interactions involved in these parameters are not the same. Equation (1) is valid whether the tendon is undergoing elastic or plastic deformation,

**Table 1** *Mechanical properties of tail tendons from the C57BL6 mouse*

| | $\sigma$ (MPa) | $E$ (MPa) | $u$ (MPa) | $u_p$ (MPa) | $\varepsilon$ |
|---|---|---|---|---|---|
| Control | 55.0 ± 4.9 | 434.2 ± 39.5 | 6.1 ± 0.7 | 2.5 ± 0.9 | 0.199 ± 0.008 |
| M20 | 59.0 ± 3.4 | 534.0 ± 28.3 | 6.3 ± 0.5 | 1.8 ± 0.2 | 0.184 ± 0.005 |
| M80 | 79.5 ± 9.7* | 644.5 ± 71.7* | 10.0 ± 1.6* | 1.4 ± 0.2 | 0.202 ± 0.011 |

M20 = samples treated at −20°C; M80 = samples treated at −80°C.
Values are mean ± s.e. ($n = 10$).
*Significant difference of treatment (with respect to the control) at $P < 0.05$.

which is determined by the forces of interactions between the GAGs of decorin PGs on adjacent collagen fibrils. Equation (2) is only valid when the tendon is experiencing plasticity, which could involve the plastic deformation of fibrils and the breaking of covalent bonds between collagen molecules in the fibril. Thereafter, the broken bonds could inhibit the motion of collagen molecules around the dislocations, leading to a strengthened tissue as energy of the remaining bonds increases and the bond length contracts (Sun, 2009).

It follows that any increase in $E$ is regulated by the van der Waals (VDW) forces between GAGs from collagen-bound PGs, at adjacent fibrils. The interactions are significant for as long as the fibrils are in close proximity to one another. During freezing, as water withdraws from the water compartment, beginning in the PG matrix (Bevilacqua *et al*., 1979), and precipitates into ice crystallites, the ion concentration increases in the non-water compartment (Muldrew and McGann, 1990), creating a concentration gradient across the unfrozen zone. As cations (e.g. $Na^+$) diffuse to the anionic charge of the GAGs, the increase in the concentration of cations around the GAGs increases the attractive forces between the GAGs. This effect may be appreciable at −80°C but not at −20°C. Moreover, the changes occurring in the tendons from the M80 group may not be completely reversible during thawing; in this case, a greater GAG–GAG interaction increases the resistance for fibril–fibril sliding when the tissue is stretched so that the tissue becomes stiffer than unfrozen ones. To understand how this could have happened, a molecular model was developed to study GAG–GAG interactions (following from Redaelli *et al*., 2003). Mobile cations, namely $Na^+$, were designated in closed proximity to each group to model a hypertonic PG matrix environment; the number of $Na^+$ ($M$) was varied to investigate the effects on the VDW energy, which was evaluated as a function of the distance between the PG molecules, $\delta$. The model was solved by molecular mechanics using software Hyperchem (Version 7.5, Hypercube Inc., Florida, USA). It was found that VDW energy, which decreased as $\delta$ increased, was affected by $N$. In particular, VDW energy increased by about 1.2 times as $N$ increased twofold, but the profile of the energy-$\delta$ curves was not affected. Further details can be found in supplementary material. Thus, we concluded that the overall effect of freezing led to a localisation and densification of charge and energy. Hence, $E$ has to be increased as predicted by equation (1).

Any increase in $\sigma$ could be attributed to changes in the packing of collagen molecules in the fibril. Low storage temperature could alter the long-range order of radial packing of collagen molecules, which could be assessed by the diffuse-scattering region from X-ray diffraction patterns of these tissues. Changes to the diffuse region occur during freezing; tissues frozen at −150°C exhibit reduced diffuse regions suggesting that the long range order is increased (Laing *et al*., 2003). Whether the effect is reversible upon thawing is not clear; Hickey and Hukins (1979) had shown that thawed tissues (frozen at −35°C) exhibited smaller diffuse regions as compared with control samples. An increase in the long-range order implies that the fine structure, that is, the crystalline arrangement of collagen molecules, of the fibril would have to be disturbed to a very much greater depth. More molecules would be involved in absorbing the energy needed to cause fibril rupture; thus more energy is absorbed by the tissue. As pointed out earlier in this section, stresses will not concentrate at regions near to the fibril surface, an important factor determining the failure of fibrils. Instead, stresses will be distributed deeper within the fibril, thus making the fibril less susceptible to fracture so that a higher $u$, and consequently higher $\sigma$ as predicted by equation (2), would be needed to rupture the tendon.

We note that $u_p$ is not affected by low storage temperatures. This suggests that low storage temperature did not have a significant effect on the molecular interaction at the fibril–PG interface and in the bulk of the PG matrix. We also note that the extensibility of the tendon, which is parameterised by $\varepsilon$, was not sensitive to low storage temperatures. We recalled that X-ray diffraction patterns of stretched tendons revealed that the tissue strain would always be larger than the strain within the collagen fibrils (Puxkandl *et al*., 2002). It is possible that the changes affecting the strain in individual fibrils would have negligible influence on the overall strain at maximum stress in the tissue stored at sub-zero temperature.

The purpose of this paragraph is to discuss the effects of cooling on the size of the ice crystallites formed in the tendons. According to Bevilacqua *et al*. (1979), a combination of the effects of solute concentration (due to an increase in viscosity) and thermal gradients (due to latent heat release and heat lost from the unfrozen zone), in the region between the crystallites, could lead to super-saturation and supercooling. Theoretically, the cooling rate of the tissue is proportional to the square of the moving speed of the freezing

front, $u^2$, while the temperature gradient at the solid-liquid interface ($G$) is proportional to $u$ (Miyawaki *et al.*, 1992). Here, $G = T_m - T_s/x$ where $x$ is the length of the frozen crystallite and $T_s$ and $T_m$ are the operating temperature of the freezer and the temperature at the surface of the crystallite, respectively. Empirically, the thickness ($d_p$) of ice crystallites is related to $u$ and $G$; this relationship can be represented as

$$d_p \propto 1/\sqrt{uG} \quad (3)$$

Tiller and Rutter (1956). It follows that the cooling rate is related to $d_p$ in equation (3). Thus, slow freezing rates cause ice to grow in extracellular locations, resulting in large crystallites and maximum dislocation of water; rapid cooling produces small ice crystallites in both cells and ECM (Bevilacqua *et al.*, 1979). In particular, slow cooling rates correspond to wider spread of sizes; fast cooling rates correspond to narrower spread of sizes and the crystallite growth is more organised (Pardo *et al.*, 2002). Consider a model of the crystallite in the tendon. On the basis of the results of Bevilacqua *et al.* (1979) and Chevalier *et al.* (2000), using an order of magnitude estimate, we find $x \sim 100$ μm. Owing to convection in the freezers, we may approximate $T_s \sim T_f, = 0$°C, the freezing temperature of water. With these values, equation (3) was evaluated for the upper limit (0.41 mm/s; Miyawaki *et al.*, 1992) and lower limit (0.06 mm/s; Chevalier *et al.*, 2000) of $u$, that is, corresponding to four combinations, for each case of $T_m = -20$°C and $-80$°C. By determining the ratio $d_p|_{-20°C}/d_p|_{-80°C}$, this simple analysis predicts that the ice crystallites formed at the higher freezer temperature are bigger than those formed at the lower freezer temperature by 1.16 to 3.46 times. In this case, the more organised smaller crystallites are dispersed uniformly within the interfibrillar matrix, raising the ion concentration around the GAGs. This argument complements an earlier suggestion that the increase in GAG interactions, arising from a localisation and densification of charge and energy around the GAGs associated with collagen fibrils, yields a higher $E$.

In conclusion, ultra-low storage temperature affects only $\sigma$, $E$ and $u$ in tail tendons from the C57BL6 mouse, leading to tissues with larger $\sigma$, $E$ and $u$. The results of this study imply that care is required when considering the method for storing and preserving tendons in order to minimise changes to the elasticity of the tissue.

## Acknowledgements

CY was supported by an NTU research scholarship. This study was supported by grants from the EU Framework V, and the Merlion-France 2007 programme (from the French Ministere des Affaires Etrangeres et Europeennes).

## References

Bevilacqua A, Zaritzky N and Calvelo A 1979. Histological measurements of ice in frozen beef. Journal of Food Technology 14, 237–251.

Chevalier D, Le Bail A and Ghoul M 2000. Freezing and ice crystals formed in a cylindrical food model: part I. Freezing at atmospheric pressure. Journal of Food Engineering 46, 277–285.

Derwin KA and Soslowsky LJ 1999. A quantitative investigation of structure-function relationships in a tendon fascicle model. Journal of Biomechanical Engineering 121, 598–604.

Giannini S, Buda R, Di Caprio F, Agati P, Bigi A, De Pasquale V and Ruggeri A 2008. Effects of freezing on the biomechanical and structural properties of human posterior tibial tendons. International Orthopaedics 32, 145–151.

Goh KL, Meakin JR, Aspden RM and Hukins DWL 2005. Influence of fibril taper on the function of collagen to reinforce the extra-cellular matrix. Proceedings of the Royal Society of London B272, 1979–1983.

Goh KL, Meakin JR, Aspden RM and Hukins DWL 2007. Stress transfer in collagen fibrils reinforcing connective tissues: effects of collagen fibril slenderness and relative stiffness. Journal of Theoretical Biology 245, 305–311.

Goh KL, Holmes DF, Lu H-Y, Richardson S, Kadler KE, Purslow PP and Wess TJ 2008. Ageing changes in the tensile properties of tendons: influence of collagen fibril volume fraction. Journal of Biomechanical Engineering 130021011, 1–8.

Gondret F, Hernandez P, Remignon H and Combes S 2009. Skeletal muscle adaptations and biomechanical properties of tendons in response to jump exercise in rabbits. Journal of Animal Science 87, 544–553.

Hickey DS and Hukins DWL 1979. Effect of methods of preservation on the arrangement of collagen fibrils in connective tissue matrices: an X-ray diffraction study of annulus fibrosus. Connective Tissue Research 6, 223–228.

Hukins DWL and Aspden RM 1985. Composition and properties of connective tissues. Trends in Biochemical Sciences 10, 260–264.

Laing JH, Cameron GJ and Wess TJ 2003. Molecular organisation of collagen fibrillar structures – a review. Recent Research Developments in Molecular Biology 1, 51–71.

Laissue P, L'Hôte D, Serres C and Vaiman D 2009. Mouse models for identifying genes modulating fertility parameters. Animal 3, 55–71.

Lin TW, Cardenas L and Soslowsky LJ 2004. Biomechanics of tendon injury and repair. Journal of Biomechanics 37, 865–877.

Miyawaki O, Abe T and Yano T 1992. Freezing and ice structure formed in protein gels. Bioscience, Biotechnology and Biochemistry 56, 953–957.

Moussa M, Babilé R, Fernandez X and Remignon H 2007. Biochemical and biomechanical properties of tendons in two commercial types of chickens. Animal 1, 983–988.

Muldrew K and McGann LE 1990. Mechanisms of intracellular ice formation. Biophysical Journal 57, 525–532.

Pardo JM, Suess F and Niranjan K 2002. An investigation into the relationship between freezing rate and mean ice crystal size for coffee extracts. Trans IChemE – Food and Bioproducts Processing 80, 176–182.

Puxkandl R, Zizak I, Paris O, Keckes J, Tesch W, Bernstorff S, Purslow P and Fratzl P 2002. Viscoelastic properties of collagen: synchrotron radiation investigations and structural model. Philosophical Transactions of the Royal Society of London B357, 191–197.

Redaelli A, Vesentini S, Soncini M, Vena P, Mantero S and Montevecchi FM 2003. The possible role of decorin glycosaminoglycans in fibril to fibril force transfer in relative mature tendons – a computational study from molecular to microstructural level. Journal of Biomechanics 36, 1555–1569.

Screen HRC, Chhaya VH, Greenwald SE and Bader DL 2006. The influence of swelling and matrix degradation on the microstructural integrity of tendon. Acta Biomaterialia 2, 505–513.

Sikoryn TA and Hukins DWL 1988. Failure of the longitundinal ligaments of the spine. Journal of Materials Science Letters 7, 1345–1349.

Sun CQ 2009. Thermo-mechanical behavior of low-dimensional systems: the local bond average approach. Progress in Materials Science 54, 179–307.

Tiller WA and Rutter JW 1956. The effect of growth conditions upon the solidification of a binary allow. Canadian Journal of Physics 34, 96–121.